UCRL-10627

University of California

Ernest O. Lawrence Radiation Laboratory

DISLOCATIONS AND PLASTIC WAVES

Berkeley, California

DISCLAIMER

UCRL-10627

UNIVERSITY OF CALIFORNIA
Lawrence Radiation Laboratory
Berkeley, California

Contract No. W-7405-eng-48

DISLOCATIONS AND PLASTIC WAVES

John E. Dorn and S. L. Rajnak

March 1963

UCRL-10627

DISLOCATIONS AND PLASTIC WAVES

John E. Dorn[1] and S. L. Rajnak[2]

To be presented at the

International Conference on Production Engineering Research

Pittsburgh, Pennsylavania

September 9-12, 1963

(1) Miller Professor of Materials Science (1962-1963) Department of Mineral Technology and Research Metallurgist of the Lawrence Radiation Laboratory, University of California, Berkeley, California.

(2) Mathematician of the Lawrence Radiation Laboratory, University of California, Berkeley, California.

Dislocations and Plastic Waves

1. Introduction

The mathematical theory for plastic wave propagation provides the essential basis for understanding the machinability and formability of materials at high rates of strain. All theories of plastic wave propagation are contained in, or are extensions of, the classical theory that was developed independently by von Karman[1] and Taylor[2]. Since the time of the original formulation of this theory in 1942, substantial strides have been made in our understanding of the role of dislocations in the plastic deformation of crystalline materials. It is the purpose of this review to summarize some of the major contributions of dislocation concepts to the understanding of plastic wave phenomena.

2. Von Karman and Taylor Theory for Plastic Wave Propagation

All mathematical theories for plastic wave propagation are based on the equations for conservation of momentum and the conditions for continuity. For the simplest example of a plastic wave moving down a very thin rod, these equations are:

	Continuous Variations		Hugoniot Shock Conditions	
Condition for Continuity	$\frac{\partial \varepsilon}{\partial t} = \frac{\partial v}{\partial x}$	(1a)	$[\varepsilon]\frac{\partial x}{\partial t} = -[v]$	(1b)
Conservation of Momentum	$\frac{\partial \sigma}{\partial x} = \rho \frac{\partial v}{\partial x}$	(2a)	$[\sigma] = -\rho[v]\frac{\partial x}{\partial t}$	(2b)

where

ε = axial engineering strain
τ = time
v = particle velocity
α = Lagrangian coordinate along axis of rod
σ = axial engineering stress
ρ = density
$[\ ]$ = a shock in the bracketed variable

Equations 1b and 2b reveal that the velocity, $\frac{d\alpha}{dt}$, of a shock along the rod is

$$\frac{d\alpha}{d\tau} = \sqrt{\frac{1}{\rho}\frac{[\sigma]}{[\varepsilon]}} \tag{3}$$

Since Eqs. 1 and 2 contain three dependent variables (σ, ρ and v), the solution of the problem requires a third equation representing the plastic behavior of the material of the rod. In their classical development of plastic wave theory, von Karman and Taylor assumed that the stress was exclusively a function of the total strain according to

$$\sigma = \sigma(\varepsilon) \tag{4}$$

Consequently, assuming a large shock to be composed of a series of small shocks, $[\sigma]/[\varepsilon] = d\sigma/d\varepsilon$, and the velocity of propagation of the stress is given by

$$\frac{d\alpha}{d\tau} = \sqrt{\frac{1}{\rho}\frac{d\sigma}{d\varepsilon}} \tag{5}$$

When the stress level is below the yield strength, $\frac{d\alpha}{d\tau} = c = \sqrt{\frac{E}{\rho}}$, namely the velocity of an elastic wave. But when the strains are plastic, the velocity of propagation is dependent on the slope of the stress-strain curve.

Although good agreement between the experimental facts and predictions based on the von Karman and Taylor assumption is obtained occasionally, most of the available evidence suggests that the assumption is not always valid: (1) The flow stress of most materials increases as the strain rate is increased suggesting that $\sigma = \sigma(\varepsilon, \dot{\varepsilon})$, where $\dot{\varepsilon}$ is the strain rate, (2) Duwez and Clark[3] noted that the stress-time records at the end of impacted rods gave more rapid rates of propagation of stress than those deduced from theory. (3) Lee[4] also pointed out that strains near the impacted end of the bar did not exhibit the uniform maximum strain, as demanded by theory, but rather showed decreasing strains with increasing distance from the impacted end, as would be expected when the flow stress is sensitive to the strain rate, (4) Several investigators[5,6,7] independently demonstrated that even when rods were preloaded well into the plastic range, the stress resulting from a superimposed impact moved down the bar not as dictated by the slope of the stress-strain curve but rather with the velocity of an elastic wave, (5) Using Kolsky's thin wafer technique, Hauser, Simmons and Dorn[8] showed that the flow stress of pure polycrystalline Al is sensitive to the strain rate.

On the other hand, some investigators appear to have demonstrated the validity of the von Karman and Taylor assumptions. In his recent summary, Cristiescu[9] has shown that a sharp dicotomy of opinion exists between European investigators as to the possible importance of strain-rate sensitivity of the flow stress to plastic wave theory. It will be shown in the following sections that some of these issues can be resolved in terms of dislocation concepts.

3. Dislocations and Shocks in Strain

Crystalline materials deform plastically by means of motion of dislocations. In order to obtain a shock in strain as a result of a shock in stress, dislocations must jump instantly from one position to another. This, of course, is theoretically impossible. The same conclusion follows from the more sophisticated developments of Frank[10] and Eshelby[11], who have shown that the energy, Γ, per unit length of a dislocation moving at a constant velocity, v, is given by the relativistic equation

$$\Gamma = \Gamma_0 \left(1 - \frac{v^2}{c^2}\right)^{-\frac{1}{2}} , \qquad (6)$$

where Γ_0 is the rest energy and c is the velocity of sound. For this reason dislocations have inertia. A dislocation initially at rest will, the instant it is subjected to a shock in stress, retain zero velocity. It will, however, accelerate as it moves, and, in the absence of other velocity sensitive energy dissipative mechanisms it will eventually approach the velocity of sound. No shock in strain is induced as a result of a shock in stress and therefore the von Karman and Taylor assumption appears to be invalidated. This suggests that Eq. 4 should be replaced by

$$d\dot{\varepsilon} = p(\sigma,\varepsilon,\dot{\varepsilon})d\sigma + q(\sigma,\varepsilon,\dot{\varepsilon})d\varepsilon + r(\sigma,\varepsilon,\dot{\varepsilon})d\tau \qquad (7)$$

in order to account for the acceleration of dislocations.

The inertia of dislocations, however, is very small and dislocations accelerate very rapidly. If no velocity dependent dissipative forces are operative, the accelerative period can be established by equating the rate at which work is done to the rate of increase in energy of a moving dislocation. Accordingly

$$(\tau - \tau^*) b v = \frac{d\Gamma}{d\tau} \qquad (8)$$

where τ is the applied shear stress and τ^* is the velocity independent back stress acting on the dislocation. Integrating Eq. 8 gives

$$(\tau-\tau^*)\,b\,c\,\tau = \frac{\Gamma_0}{c^2}\,\frac{v}{\sqrt{1-\frac{v^2}{c^2}}} \quad . \tag{9}$$

As an illustration, we take the values appropriate of Al of $c = 5.05 \times 10^5$ cm/sec, $b = 2.86$ Å, and $\Gamma_0 = \frac{Gb^2}{2} = 1.1 \times 10^{-4}\ \frac{\text{ergs}}{\text{cm}}$, where G is the shear modulus of elasticity. Then for a very small stress of $\tau - \tau^* = 10^8$ dynes/cm^2 a dislocation will reach a velocity of $.9c$ in $\tau = 2\times10^{-11}$ sec. The shear strain at this time is given by

$$\gamma = \int_0^{\tau} \rho b v\, d\tau = 1.4 \times 10^{-4}/\text{sec},$$

where ρ, the density of the dislocations, is taken to be 10^8 per cm^2. A more sophisticated analysis of the behavior of a Frank Read source under impact[12] gives about the same general answer: Inertias of dislocations are so small that they reach almost their relativistic velocities in 10^{-10} sec., even for low stresses. At this time the plastic strain is yet very small. Therefore, except for problems where very short times and very small plastic strains are significant, the acceleration of dislocations can be neglected in formulating the mathematical theory for plastic wave propagation. Consequently the material behavior for plastic wave theory can most frequently be described in terms of the empirical relationship

$$d\varepsilon = h(\sigma,\varepsilon)\,d\sigma + g(\sigma,\varepsilon)\,d\tau \quad . \tag{10}$$

The function h refers to the ratio of a small shock in strain as a result of a small shock in stress and g gives the plastic strain rate under a constant stress. The detailed functions to be employed in Eq. 10, however, should be

rationalized in terms of dislocation theory.

As shown in Table I, dislocation mechanisms are conveniently classified into three major categories:

Table I

Classes of Dislocation Mechanisms

Class	Class Name	Examples	Characteristics
I	Athermal (activation energies greater than 50kT)	1. Long Range Stresses 2. High Local Stresses 3. Short Range Order Alloys 4. Suzuki Locked Alloys	Flow stresses that are insensitive to temperature and independent of strain rate. $\frac{\tau}{G} \approx f(\gamma)$ (G = Shear Modulus)
II	Thermally Activated Processes (activation energies less than 50kT)	1. Peierls Process 2. Intersection 3. Cross slip 4. Motion of Jogged Screws 5. Climb of Edges 6. Viscous creep due to Solute Atom Interactions	Flow stress that decreases rapidly with an increase in temperature or a decrease in strain rate. $\dot{\gamma} \propto \exp(-\frac{u}{kT})$ where $u = u(\tau, T, str)$ str = structure and T = absolute temperature
III	Phonon Scattering Other velocity sensitive processes that are not thermally activated	Liebfried Reaction ----------	$\dot{\gamma} \propto \frac{(\tau - \tau^*)}{T}$ ---------

The value of this classification arises from the differences in the effect of strain rate and temperature on the flow stress as shown in the last column of the table. Occasionally only one process in one class is operative. But often under dynamic test conditions several athermal processes, several thermally activated processes, as well as the phonon scattering mechanism, etc., may simultaneously contribute to the observed mechanical behavior of crystalline materials. The only generalization that can be made, here, concerns the fact that the creep mechanisms that depend on diffusion such as the motion of jogged screw dislocations, climb of edge dislocations and the viscous drag of solute atom atmospheres are usually so slow that they do not play a role in the dynamic behavior of materials at high strain rates. In the following sections of this report several special cases of dislocation processes under dynamic conditions will be discussed.

4. Behavior of a Suzuki Locked Alloy

A typical resolved shear stress-shear strain diagram for basal slip on single crystals of the hexagonal phase containing 67 atomic percent Ag and 33 atomic percent Al, when tested in slow tension, is shown in Fig. 1. The yielding begins gradually at a well-rounded upper yield point, at which a single Luder's band having the exceptionally large Luder's strain of $\gamma = 1.35$ is formed. Following migration of the Luder's strain over the gage section only modest amounts of strain hardening are obtained. The upper and lower yield points that were obtained in a series of slow and dynamic tests are shown in Fig. 2. These data reveal that, within the experimental accuracy, the upper and lower yield stresses are insensitive to the strain rate; furthermore, they increase with an increase in temperature even as the temperature approaches the melting point. Obviously the dislocation mechanism that is

involved is not thermally activated, and the only non-thermally activated process known that can exhibit a yield point is Suzuki locking. The increase in flow stress with temperature can arise from one or from both of two independent factors; under certain conditions the effectiveness of Suzuki locking can increase with an increase in temperature and, under all conditions, high speed dislocations will interact with phonons.

Suzuki has shown that for regular solid solutions at sufficiently high temperatures (above about 0.4 of the melting temperature), where an equilibrium distribution of solute atoms between the stacking fault and the surrounding crystal is obtained, the flow stress, τ, is given by

$$\tau = \frac{2h}{Vb} H c_o(1-c_o) \frac{1 - \exp(-\frac{H}{RT})}{1 - c_o(1 - \exp(-\frac{H}{RT}))} \qquad (11)$$

where

$$H = \frac{V}{2h}(\gamma_a - \gamma_b) \qquad (12)$$

b = the Burger's vector
V = the molar volume of the alloy
h = the height of one atomic layer
γ_b = the stacking fault energy of pure b
γ_a = the stacking fault energy of pure a
Co = the mole fraction of solute atoms
R = the gas constant
T = the absolute temperature

Below about $T_f = 0.4$ of the melting temperature, the composition in the stacking fault becomes frozen in. Therefore for $0 < T \leq T_f$ the value of T must be replaced by the constant temperature T_f. In this range τ acquires a constant value independent of temperature. If the difference in stacking

fault energy $\gamma_b - \gamma_a$ does not change much with temperature, or if it decreases as the temperature increases, τ will decrease somewhat as the temperature increases above T_f. But if $\gamma_b - \gamma_a$ increases sufficiently rapidly with an increase in temperature, τ will also increase as the temperatue increases above T_f. If all of the variation in the upper yield strength with temperature is attributed to Suzuki locking, the values of $\gamma_b - \gamma_a$ shown in Fig. 3 are obtained. Thermodynamic data are not available to ascertain which one of the two possible sets of values for $\gamma_b - \gamma_a$ is valid, but stacking fault energies can amount to several hundred ergs/cm^2. Consequently either of the sets of observed data are consistent with the concept of Suzuki locking.

The upper yield strength for basal slip of an HCP Suzuki-locked crystal should take place when the applied stress is slightly greater than the locking stress, τ. Unlocked dislocations, in the absence of any velocity sensitive dissipative mechanism, will travel at a speed that approaches that of sound. Those mechanisms for the multiplication of dislocations, such as cross slip, which are operative in BCC and high stacking fault energy FCC metals are not expected to be operative for basal slip in the hexagonal system.

At the higher temperatures of test, however, phonon scattering should serve to limit the velocity of the liberated dislocations. Attempts by Liebfried,[15] Nabarro[16] and Eshelby[17] to rationalize the effect of phonon scattering on the velocities of dislocations have served to reveal the complexity of the problem. Liebfried, however, has suggested that the dislocation velocity, v, in the absence of relativistic complexities, might be approximated by

$$v = \frac{10 \lambda^3 c \tau}{3kT} , \qquad (13)$$

provided $v/c < 1$.

In view of the very large Luder's strain that is obtained in slow tension tests, it must be assumed that the back stresses on released dislocations is very small and the dislocations are subjected to a net stress that is only slightly less than the upper yield strength. Introducing the experimentally determined values of τ and T for the upper yield stress into Eq. 13, we obtain $v/c \approx 10^{6}$. Thus we judge that damping due to interaction of phonons and dislocations is not significant in this example.

If ρ is the density of moving dislocations,

$$\dot{\gamma} = \rho b v . \tag{14}$$

Assuming $v = c$ for the released dislocations we estimate that ρ at the upper yield strength has the reasonable values ranging from $\rho = 2 \times 10^{4}/cm^{2}$ at $\dot{\gamma} = 300$ to $\rho = 5 \times 10^{6}$ at $\dot{\gamma} = 60{,}000/sec$.

We now attempt to ascertain how Eq. 10, for use in plastic wave theory, might be formulated for this case. We will assume that the least time that can be measured experimentally is 10^{-6} sec. In this interval of time at the strain rate of 10^{4} per sec. the plastic strain is only 0.01. If our interest is in much larger plastic strains, we might neglect this small plastic strain. In that event we might write Eq. 10 as

$$d\varepsilon = \frac{d\sigma}{E} + \rho b \ell \, d\tau \tag{15}$$

where ρ, the density of the released dislocations, is somewhat undetermined function of the stress and strain. If however ρ is larger than 10^{6} per cm^{2}, a strain larger than 0.01 will be obtained within the selected least time count of 10^{-6} sec. Although Eq. 15 will still be valid, the data will appear t indicate an instantaneous plastic strain as suggested by the von Karman and Taylor assumption.

5. Peierls Process

When single crystals of the 67 atomic percent Ag and 33 atomic percent Al are so oriented as to slip on the prismatic plane, they no longer show a yield point and exhibit only a modest rate of strain hardening. The initial flow stresses that are obtained depend on temperature as shown in Fig. 4. For slow tension tests, three regions are clearly delineated: (I) A region from 0° to about $150^{\circ}K$ over which the flow stress decreases precipitously with an increase in temperature. Since the activation volume was observed to be about $15b^3$, this thermally activated process is thought to be the Peierls process; (II) Over the region from 150° to about $475^{\circ}K$, prismatic slip takes place by some athermal process. Since dislocations on the prism plane are undissociated, this athermal process cannot be ascribed to Suzuki locking. As demonstrated previously,[13] the only athermal process that can account for the high flow stress is that due to short range ordering; (III) In a detailed investigation[18] it has been demonstrated that the thermally activated process taking place above $475^{\circ}K$ is diffusion controlled disordering.

As shown by the dynamic test data, recorded in Fig. 4, prismatic slip appears to be controlled by a single thermally activated mechanism, namely the Peierls mechanism over the entire range of temperatures. As the strain rate is increased, higher flow stresses are obtained and the Peierls process becomes operative over the range of temperatures of Region II, where the deformation was controlled at much lower strain rates by the athermal process due to short range ordering. Furthermore, diffusion is so slow that it can only function as a possible mechanism for low strain rates. Consequently, when some critical strain rate is exceeded in Range III, slip can no longer

be controlled by diffusional processes and other mechanisms of deformation become rate controlling. A change of strain rate from 10^{-4} to 55×10^{3}/sec at 600°K caused the rate-controlling mechanism of slip to change from a diffusional process to a modified Peierls mechanism. This change in strain rate was accompanied by an increase in flow stress by a factor of 30.

The exact formulation of the Peierls mechanism is yet under development. For the purpose of the present objectives, however, a quasi-empirical formulation of the mechanism is justified. We assume that the activation energy to nucleate a pair of kinks of opposite sign is given by $u_k - (\tau - \tau^*) wb^2$, where w is the separation of the pair of kinks. Thus the frequency of formation of a kink pair, ν_m, is given by

$$\nu_m = \frac{1}{\tau_m} = \frac{\nu b}{2w} \exp\left(-\frac{u_k - (\tau - \tau^*) w b^2}{kT}\right), \quad (16)$$

where ν is approximately the Debye frequency. If no other factors are involved the strain rate is given by

$$\dot{\gamma} = \frac{\rho}{2l}(2lb) b \frac{1}{\tau}, \quad (17)$$

where $\tau = \tau_m$ and l is the free length of travel of each kink of the pair formed. This formulation is in agreement with the slow tension test data. On the other hand, it predicts too low flow stresses for the high strain rates. The Lothe-Hirth model[22] for the Peierls process gives only very slightly better agreement with the high strain rate data.

In the above formulation it was assumed that the kinks moved so rapidly once they were formed that the time, τ_m, it took for each to move a distance, l, was small. If the motion of each kink is determined by some velocity sensitive dissipative process, this time need no longer be negligible especially at the higher strain rates. Under these circumstances better agreement with

the experimental data can be expected.

Two viscous process were investigated. According to the Leibfried equation for dislocation-phonon interactions,

$$\frac{l}{\tau_m} = \frac{10 c b^3 (\tau - \tau^*)}{3 kT} . \tag{18}$$

Therefore τ of Eq. 17 is $\tau = \tau_n + \tau_m$. But introducing this value reveals that the viscous damping as a result of phonon interaction is not great enough to account for the observed results. Stronger viscous-like damping is expected when the kink motion is thermally activated. Under these conditions we expect that

$$\frac{l}{\tau_m} = \frac{\nu b}{2} e^{-\frac{u_m}{kT}} \sinh \frac{(\tau - \tau^*) b^3}{kT} \tag{19}$$

where $u_m < \mu_k$. Again using reasonable values for u_m, the predicted values did not agree well with the experimental results. This suggests that some as yet unknown strong viscous-damping mechanism is operative.

6. Thermally Activated Intersection

Seeger[19] has shown that when the plastic shear strain rate is controlled by the rate of intersection of dislocations,

$$\dot{\gamma} = N A b \nu e^{-\frac{q}{kT}} , \tag{20}$$

where

N = the number of points per unit volume of contact between the forest dislocations that are being cut and the glide dislocations

A = the average area swept out per intersection

$\mathcal{U}$ = the average energy that must be supplied by a thermal fluctuation to complete intersection.

For Al, where the dislocations are dissociated slightly into Shockley partials, the average force versus displacement diagram at the absolute zero for intersection is given by the solid intersecting curve of Fig. 5.[20] As the dislocations are brought together α decreases and F_o increases. As α decreases the dislocations first constrict, the constriction being completed at $\alpha = b$. Between $\alpha = b$ and $\alpha = 0$ jogs are produced.

At temperatures above the absolute zero, the force is given by

$$F = F_o \frac{G}{G_o} , \tag{21}$$

where G and G_o are the shear moduli at the test temperature and the absolute zero respectively. Both the constriction energy and the jog energy are linearly dependent on the shear modulus of elasticity.

If L is the mean spacing of the forest dislocations, a force

$$F = (\tau - \tau^*) L b \tag{22}$$

will act at the point of intersection where τ is the externally applied shear stress, and τ^* is the back stress due to local interactions and long range stress fields. For our present objectives it will not be necessary to separate these two effects. If a force F less than F_m is applied, the energy that must be supplied by a thermal fluctuation in order to complete intersection is

given by the modified Basinski equation

$$u = \int_{(\tau-\tau^*)Lb}^{F_m} \eta \, dF. \tag{23}$$

Equations 20 to 23 plus the data of the $F_o - \eta$ curve given in Fig. 5 then completely describe the intersection mechanism. It is significant that none of these equations contain explicitly the plastic shear strain. This arises because the shear strain itself is never a physically significant variable. Rather the physically important variables, at least for the intersection mechanisms, are the structurally significant quantities of $\tau^* = \tau_o^* \, G/G_o$ and L. In general these are not simply related to the strain but are also dependent on the temperature and strain-rate history of straining. As deduced from slow tensile tests for $\dot{\gamma} = 10^{-4}$/sec. and T = 90°K, they are given in Fig. 6.[20] When the metal is strained, L decreases and τ^* increases, both factors contributing to strain hardening.

It will prove instructive to first formulate the intersection mechanism in terms of Seeger's approximation which neglects the effects of constriction and is therefore appropriate for intersection of undissociated dislocations. For this simplification

$$u = u_o \frac{G}{G_o} - \left(\tau - \tau_o^* \frac{G}{G_o}\right) L b^2, \tag{24}$$

where the subscripts zero refer to the values at the absolute zero. This simplification arises because the $F - \eta$ diagram no longer contains the curved part of Fig. 5 due to the constriction force and is then represented by a rectangular area from $0 < F < F_m$ and $0 < \eta < b$. Introducing Eq. 24 into Eq. 20 gives

$$\tau \frac{G_o}{G} = \tau_o^* + \frac{u_o}{Lb^2} - \frac{kT\,G_o}{Lb^2 G} \ln \frac{NAbv}{\dot{\gamma}}, \quad \text{for } T < T_c \tag{25}$$

and

$$\tau \frac{G_o}{G} = \tau_o^* \quad \text{for } T > T_c \,, \tag{26}$$

where T_c is defined by

$$u_o = kT_c \ln \frac{NAbv}{\dot{\gamma}} \,. \tag{27}$$

The critical temperature, T_c, is that temperature at which the necessary thermal fluctuations needed to assist the applied stress in order to complete intersection occur practically instantaneously. Below that temperature, as shown by Eq. 25 the flow stress decreases linearly with an increase in the absolute temperature. These trends are shown in Fig. 7 for the case of a mildly strain hardened metal where, as given in Fig. 6, 1/L was selected to be $7.3 \times 10^{+5}$ 1/cm and τ^* was taken as 4.8×10^{8} dynes/cm^2. For a given $\dot{\gamma}$, T_c is known to remain insensitive to all accessible strain hardened states. Therefore NAbν is substantially a constant. In order to complete the approximation, NAbν was estimated to about 120 /sec. and U_o was approximated to be about 1.45×10^{-13} dyne-cm from Fig. 5 by neglecting the constriction energy. For $0 \leq \tau \frac{G_o}{G} \leq \tau_o^*$ the behavior is entirely elastic. And over the range $\tau_o^* \leq \tau \frac{G_o}{G} \leq \frac{u_o}{Lb^2} + \tau_o^*$ plastic deformation occurs by thermally assisted intersection, the flow stress being dependent on the strain rate. As shown by Eq. 25 the higher the test temperature, the more rapidly does the flow stress in this range increase with an increase in strain rate. Therefore tests conducted at low temperatures on only mildly strain hardened metals may have flow stresses that are substantially insensitive to the strain rate, whereas the same metal tested in a severely strain-hardened state and at higher temperatures may exhibit significantly sensitive variations of flow stress with strain rate.

An example of the effect of straining on increasing the strain-rate sensivity of dynamically tested high purity Al is shown in Fig. 8.[8] The $\log \dot{\varepsilon}$ versus σ curves, which were obtained using a modification of Kolskey[21] thin wafer technique, are less steep for the material at higher strain hardened states over the lower ranges of $\dot{\varepsilon}$ where $\ln \dot{\varepsilon}$ is linear with σ, as dictated by Eq. 25.

When $\gamma \frac{G_0}{G} > \frac{\mu_0}{Lb^2} + \gamma_0^*$, thermal activation is no longer required to assist intersection because the force F at the point of intersection now exceeds F_m and the applied stress alone is more than sufficient to effect intersection.

The dynamic behavior of Al can now be predicted up to the limit of the intersection mechanism from the data recorded in Figs. 5 and 6 and the intersection theory. Since these predictions follow directly from the previous discussion, the details will not given here except to state that the assumption was made that the material obeyed a mechanical equation of state. The predicted behavior is compared with the experimental results in Fig. 9. The correlation between the predicted values based on data obtained from slow tension tests and the dynamic data is excellent. The maximum point on the predicted curves corresponds to that point at which the stress is sufficient to insure intersection without waiting for a thermal fluctuation. And it is just at this point that an abrupt change in slope of the curves is obtained. Obviously the plastic strain rate above about 10^2/sec is controlled by some alternate mechanism. Deformation in this region might be due, for example, to the thermally aided production of vacancies as a result of the motion of jogged screw dislocations. It is a simple matter to show, however, that for this mechanism also, $\ln \dot{\varepsilon}$ would be proportional to σ, albeit with a different slope than that for the experimental facts shown in Fig. 8. It becomes obvious

that the high strain-rate effects shown in Fig. 8 cannot be ascribed exclusively to the thermally activated motion of jogged screw dislocation.

When the data is replotted on a linear graph, as shown in Fig. 10, the strain rate is seen to increase almost linearly with the stress. But the slope of this curve is at least an order of magnitude below that which would be expected in terms of the dislocation-phonon interaction mechanism. It therefore appears that other unknown velocity sensitive energy dissipative mechanisms must yet be uncovered to account for these results. This could be due to the plucking of dislocations as they move past barriers.

Summary

The major problem that is encountered in formulating a realistic mathematical theory for plastic wave propagation in crystalline materials concerns their actual plastic behavior. If times less than 10^{-10} sec and plastic strains of less than 0.001 are significant to the problem, it will be necessary to formulate the equation for plastic deformation rates in terms of the acceleration of dislocations as well as other strain rate controlling mechanisms. If longer times and larger strains are of interest however, simple formulations based on the velocity of dislocations become feasible. In this event, Eq. 10 can be written as

$$d\varepsilon = \frac{1}{E} d\sigma + g(\sigma, \varepsilon)\, d\tau ,$$

similar to the formulation first suggested on an empirical basis by Malvern.[23] The assumed functional dependence of g on the variables, however, will have to agree with the dictates of the rate controlling dislocation mechanisms. For moderate to low stresses and strain rates, the motion of dislocations is often dictated by one or several thermally activated processes. As we have

seen, some of these are well enough understood to permit estimates of g. When, however, the stress level is sufficiently high, so as to obviate the wait for thermal activation or when the process is athermal, other velocity sensitive energy dissipative mechanisms control the rate of deformation. The phonon interaction mechanism is among these, but the experimental data now available suggest that other mechanisms, such as perhaps the plucking of dislocations as they move over potential hills, are also significant. If for these cases, the strain rate decreases precipitously with strain, within the least count of time of the experimental instrumentation that is employed, it will appear as if the von Karman and Taylor assumptions are valid insofar as shock in strain will appear to have resulted from a shock in stress, within the period of least count of the instrumentation.

REFERENCES

1. T. von Karman and P. Duwez, J. Appl. Phys. 21 (1950).
2. G. I. Taylor, Scientific Papers, 1, Cambridge Press (1957).
3. P. E. Duwez and D. S. Clark, Proceedings ASTM 47, 502 (1947).
4. E. H. Lee, Deformation and Flow of Solids, Springer-Verlog, p. 129 (1956).
5. E. J. Sternglass and D. A. Stuart, J. Appl. Mech. 20, 427 (Sept. 1953).
6. B. Alter and C. Curtis, J. Appl. Phys. 27, 9, 1079 (July 1956).
7. C. Ripabelli, Soc. Expt. Stress Anal. Proc. 14, 1, 55 (Sept. 1954).
8. F. Hauser, J. Simmons and J. Dorn, Response of Metals to High Velocity Deformation, Interscience (1961).
9. N. Cristiescu, Plasticity, Proceedings of the Second Symposium on Naval Structures, Pregamon Press, (1960).
10. F. Frank and W. Read, Phys. Rev. 79, 722 (1950).
11. J. Eshelby, J. Appl. Phys. 24, 176 (1953).
12. J. Campbell, J. Simmons and J. Dorn, J. Appl. Mech. 83, p. 447 (1961).
13. J. Mote, K. Tanaka and J. Dorn, Trans. Of Metal Soc. of AIME 221, 858 (August 1961).
14. H. Suzuki, Dislocations and Mechanical Properties of Crystals, John Wiley and Sons, p. 361-390 (1957).
15. G. Liebfried, Z. Phys. 127, 344 (1949).
16. F. Nabarro, Proc. Roy. Soc. A 209, 278 (1951).
17. J. Eshelby, Proc. Roy. Soc. A 266, 222 (1961).
18. E. Howard, W. Barmore, J. Mote and J. Dorn, "On the Thermally-Activated Mechanism of Prismatic Slip in the Ag-Al Hexagonal Intermetallic Phase", University of California, Lawrence Radiation Laboratory Publication No. 10588 (Dec. 1962).

19. A. Seeger, Phil. Mag. 1, 651 (1956).

20. S. Metra and J. Dorn, "On the Nature of Strain Hardening in Polycrystalline Al and Al-Mg Alloys", University of California, Lawrence Radiation Laboratory publication No. 10365 (July 1962).

21. H. Kolsky, Proc. Phys. Soc. London 62, 677 (1949).

22. J. Lothe and J. P. Hirth, Phys. Rev. 115, 543 (1959).

23. L. E. Malvern, Quart. Appl. Math. 8, 4, 405 (1951).

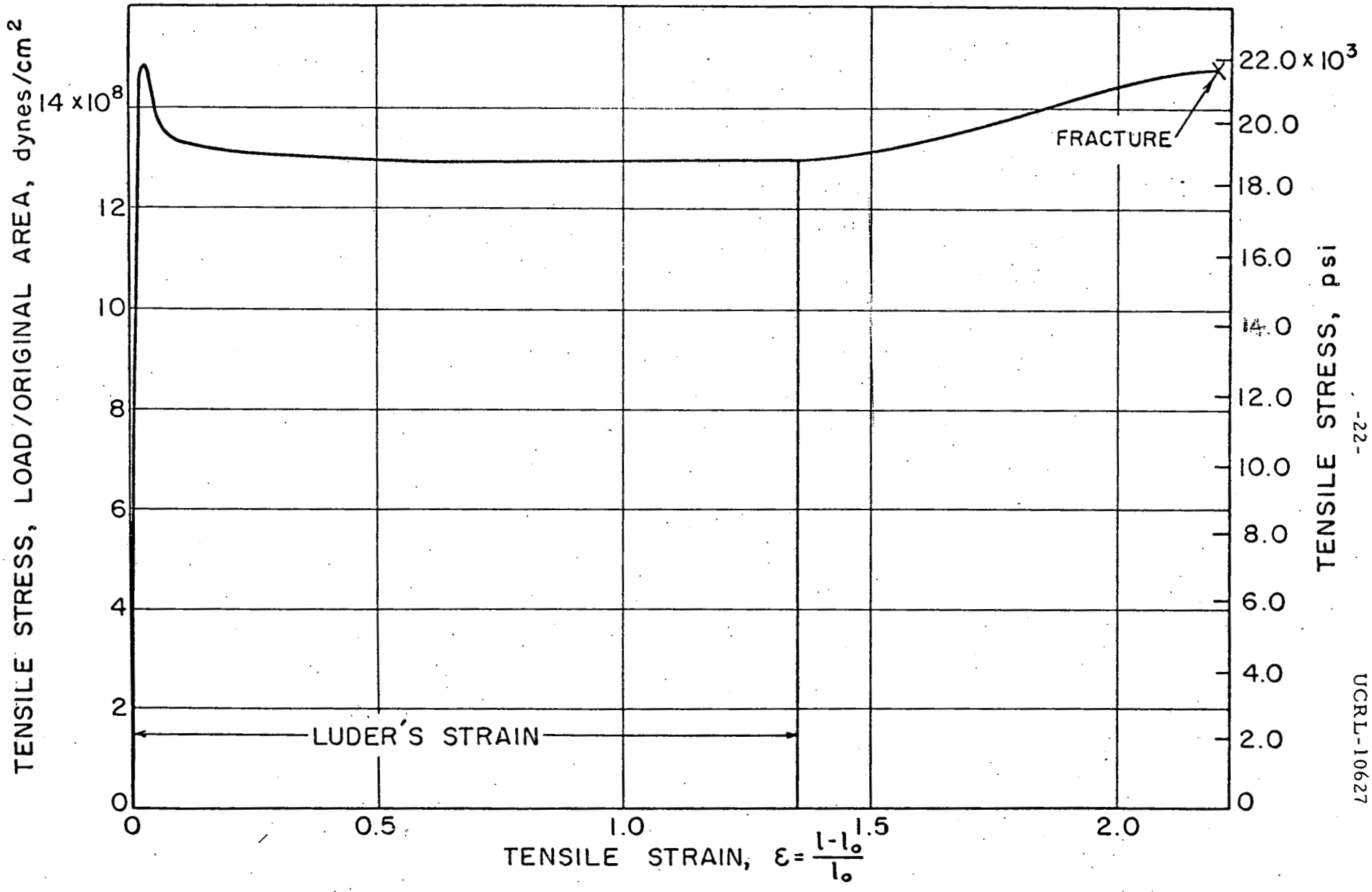

FIG. 1 TENSILE STRESS - TENSILE STRAIN DIAGRAM FOR BASAL SLIP.

UCRL-10627

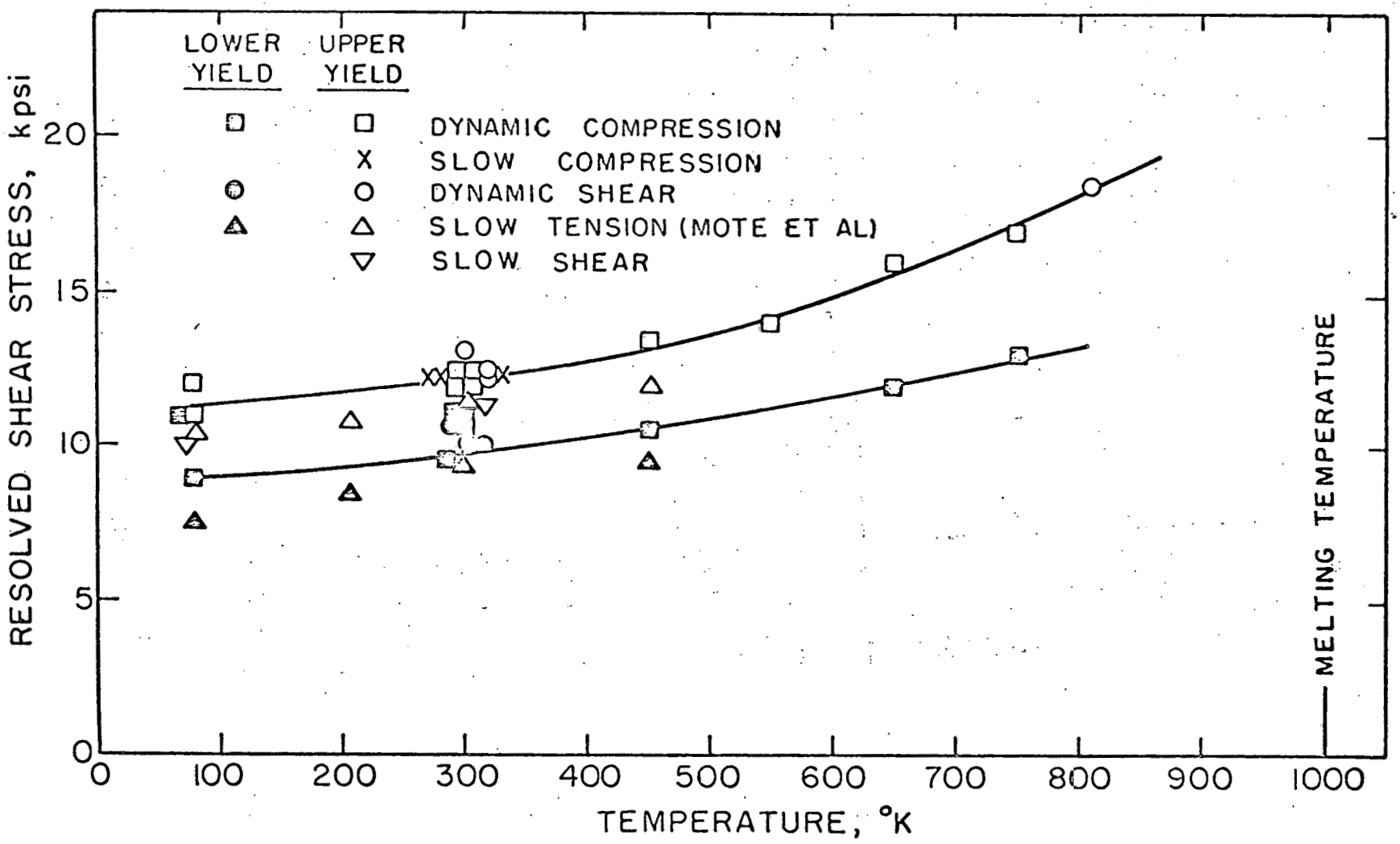

FIG. 2 RESOLVED SHEAR STRESS vs. TEMPERATURE FOR BASAL SLIP

UCRL-10627

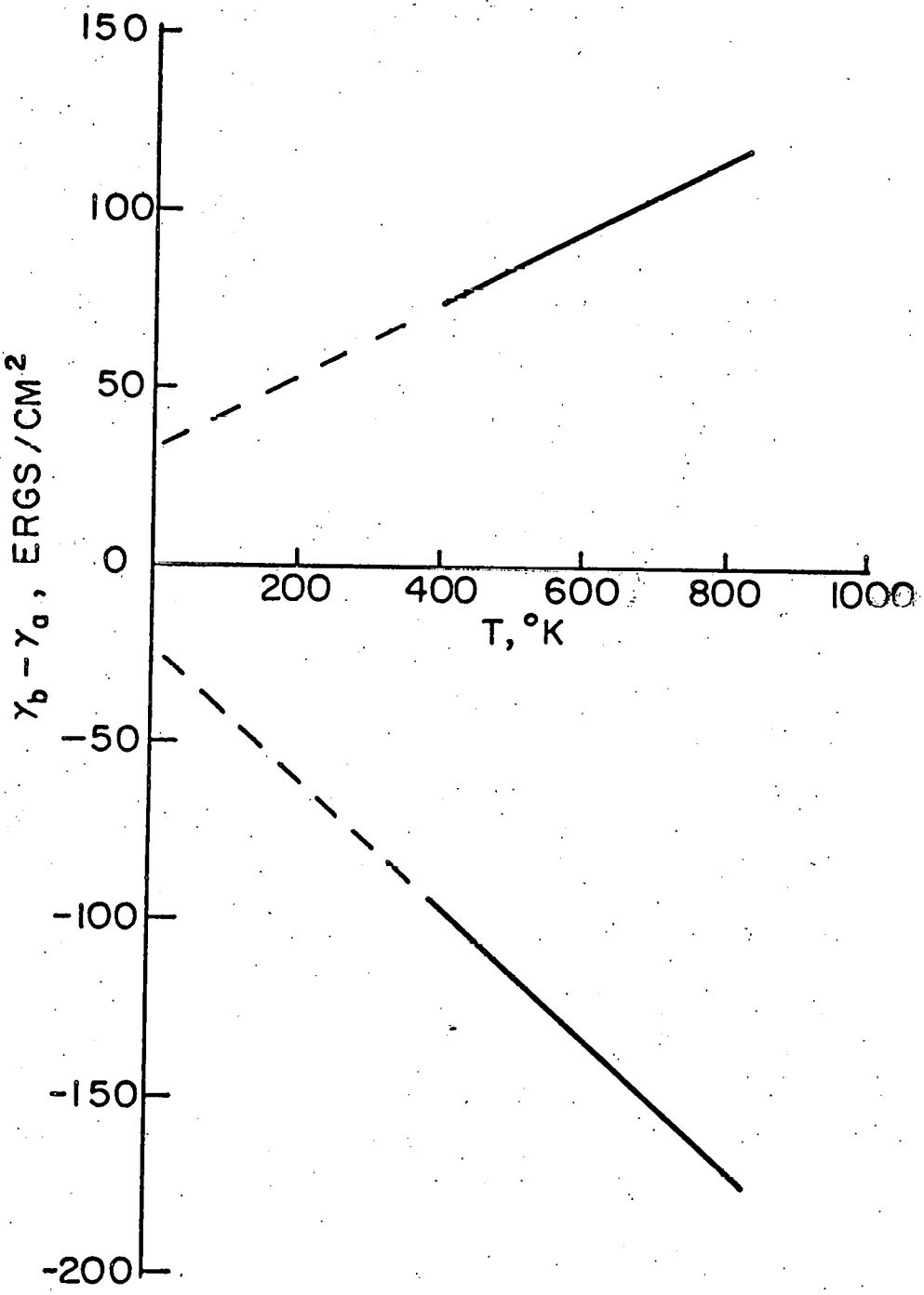

FIG. 3 $\gamma_b - \gamma_a$ vs. TEMPERATURE.

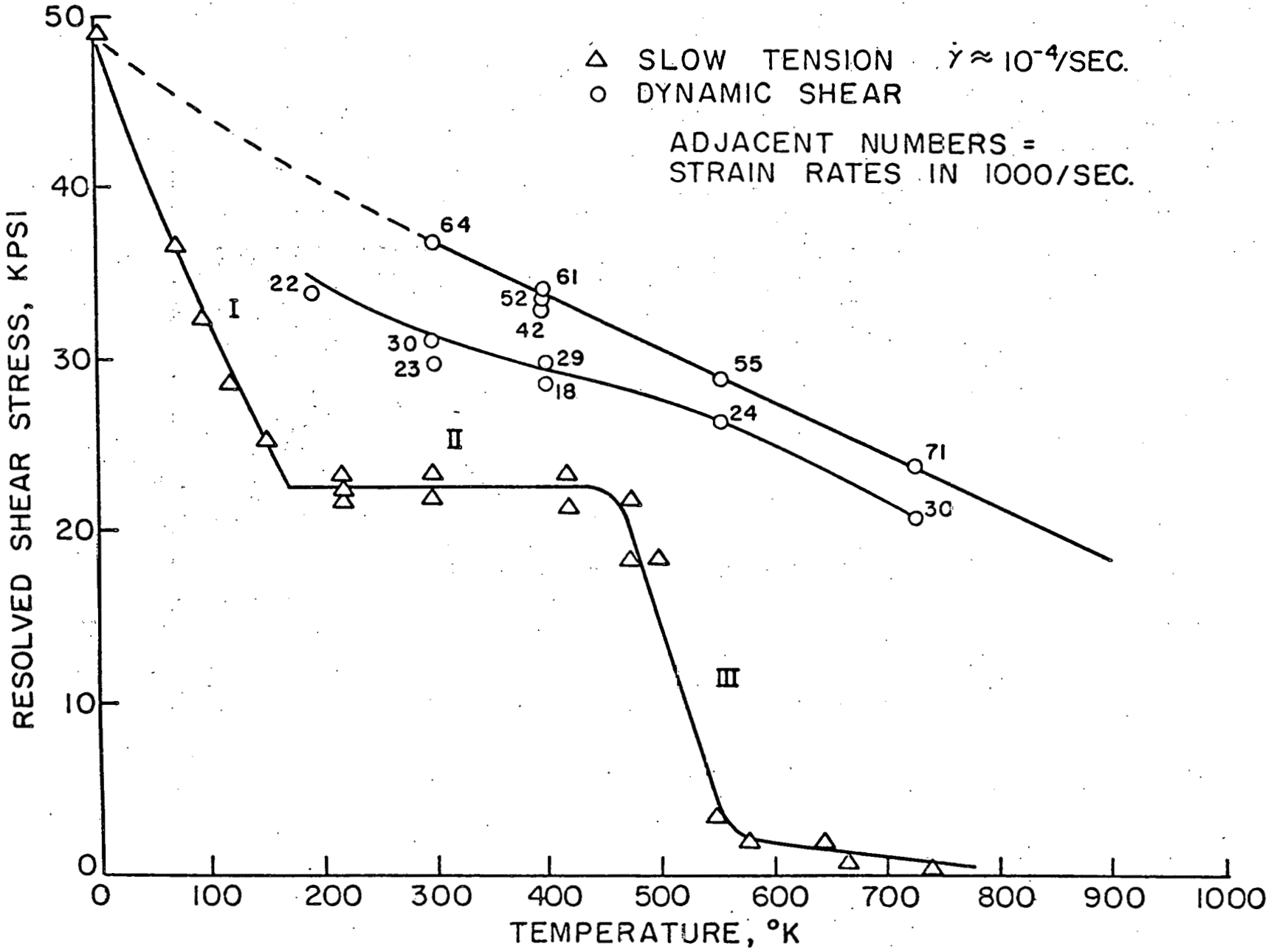

FIG. 4 PRISMATIC YIELDING OF AN Ag (67 %) - Al (33 %) ALLOY.

UCRL-10627

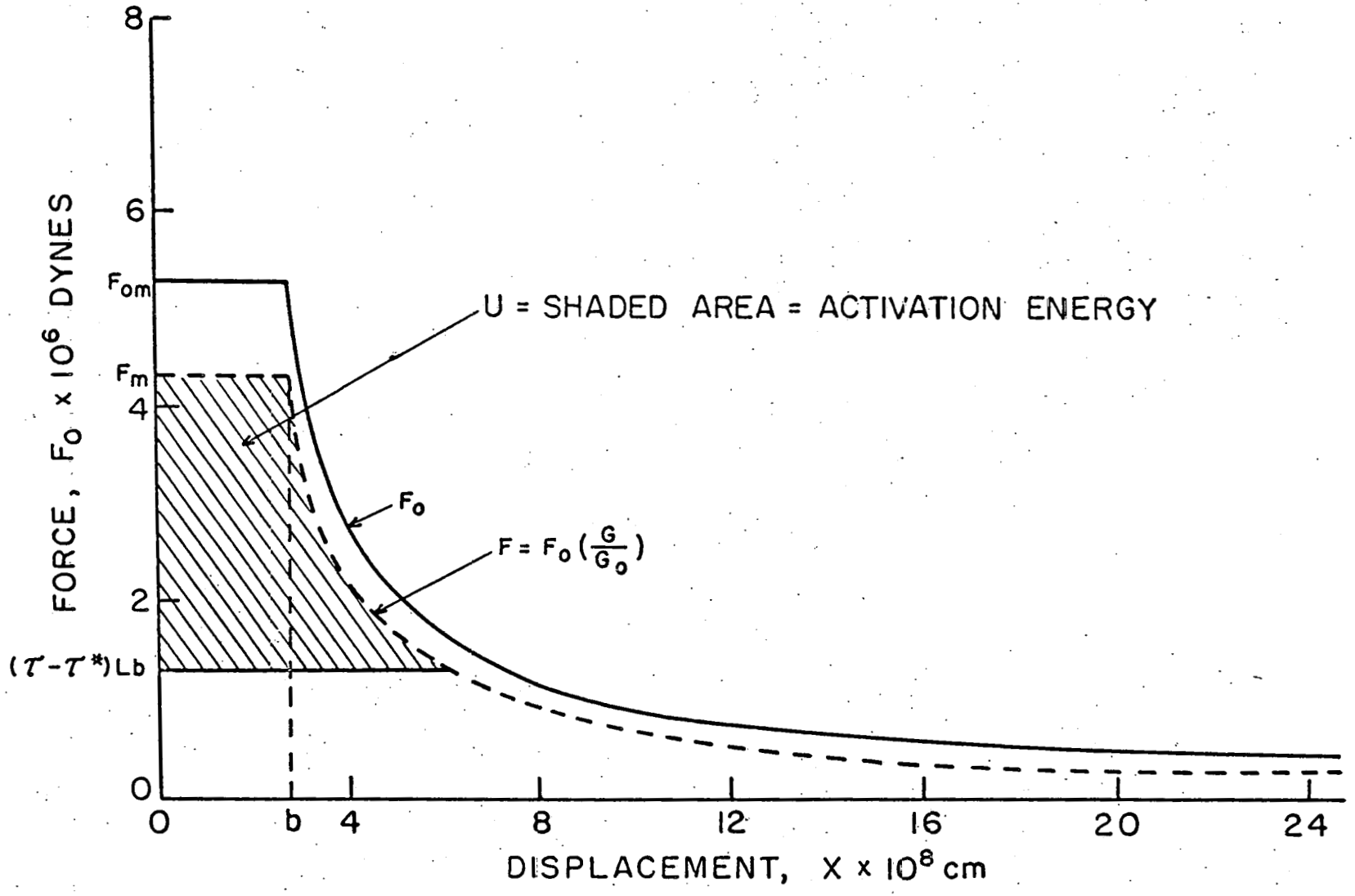

FIG. 5 FORCE - DISPLACEMENT DIAGRAM FOR INTERSECTION IN PURE Al (20).

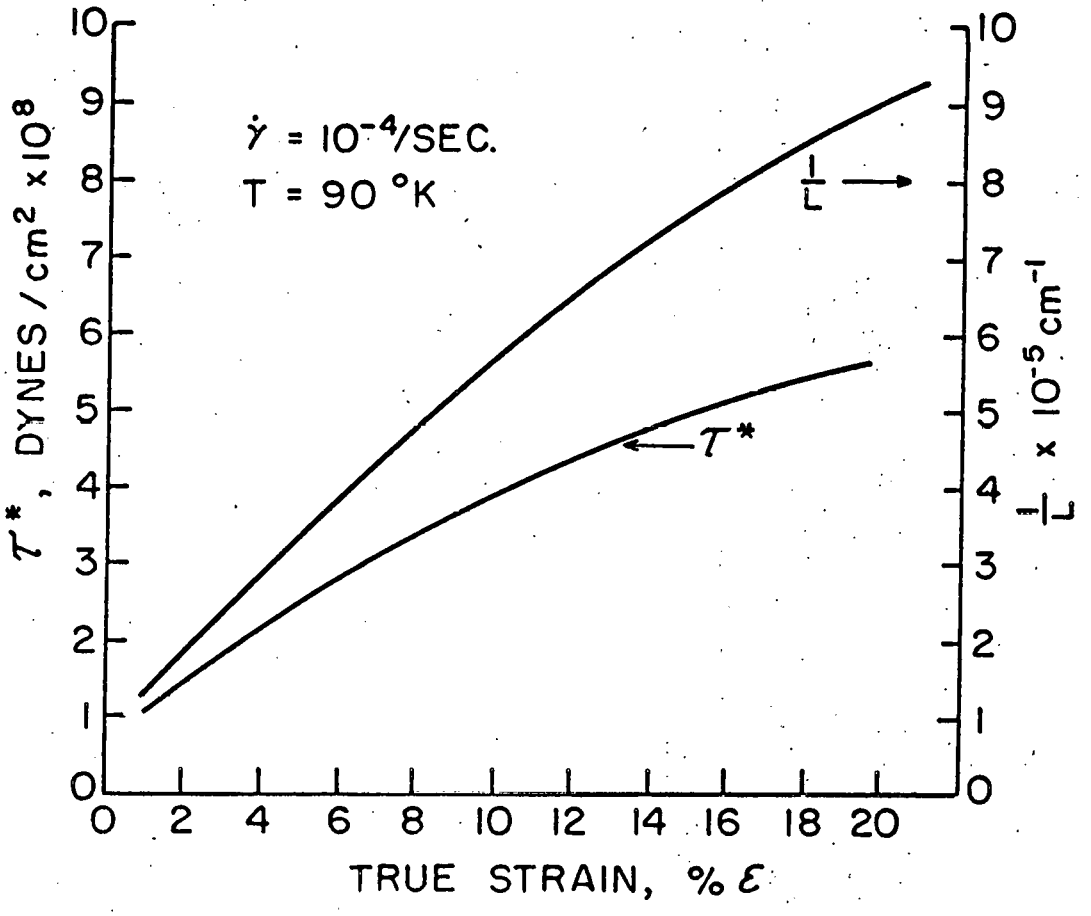

FIG. 6 VARIATION OF DISLOCATION SPACING AND BACK STRESS FIELDS WITH STRAIN IN PURE Al (20).

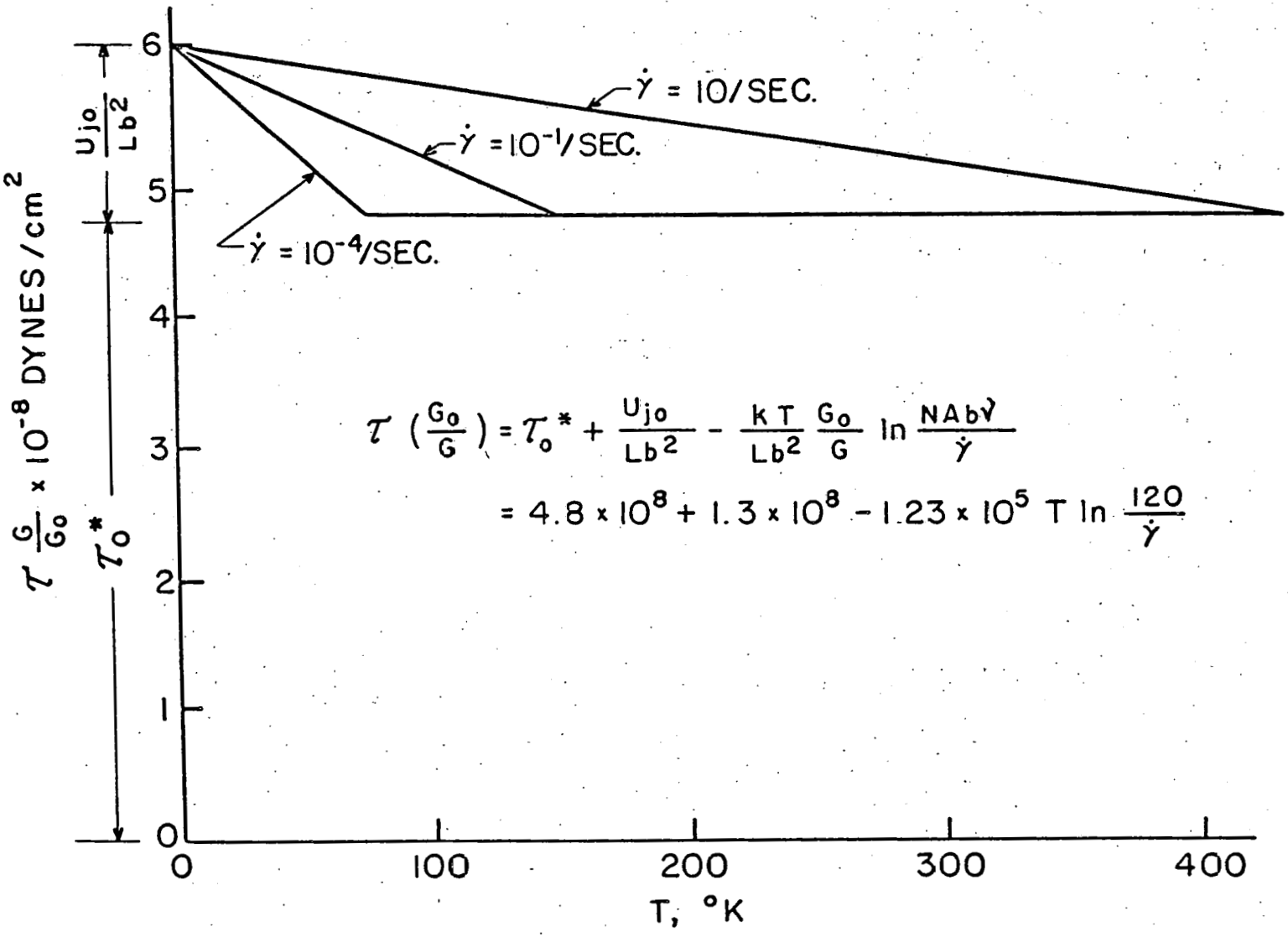

FIG. 7 REPRESENTATION OF THE STRESS-TEMPERATURE RELATION FOR INTERSECTION AT A GIVEN STRUCTURE.

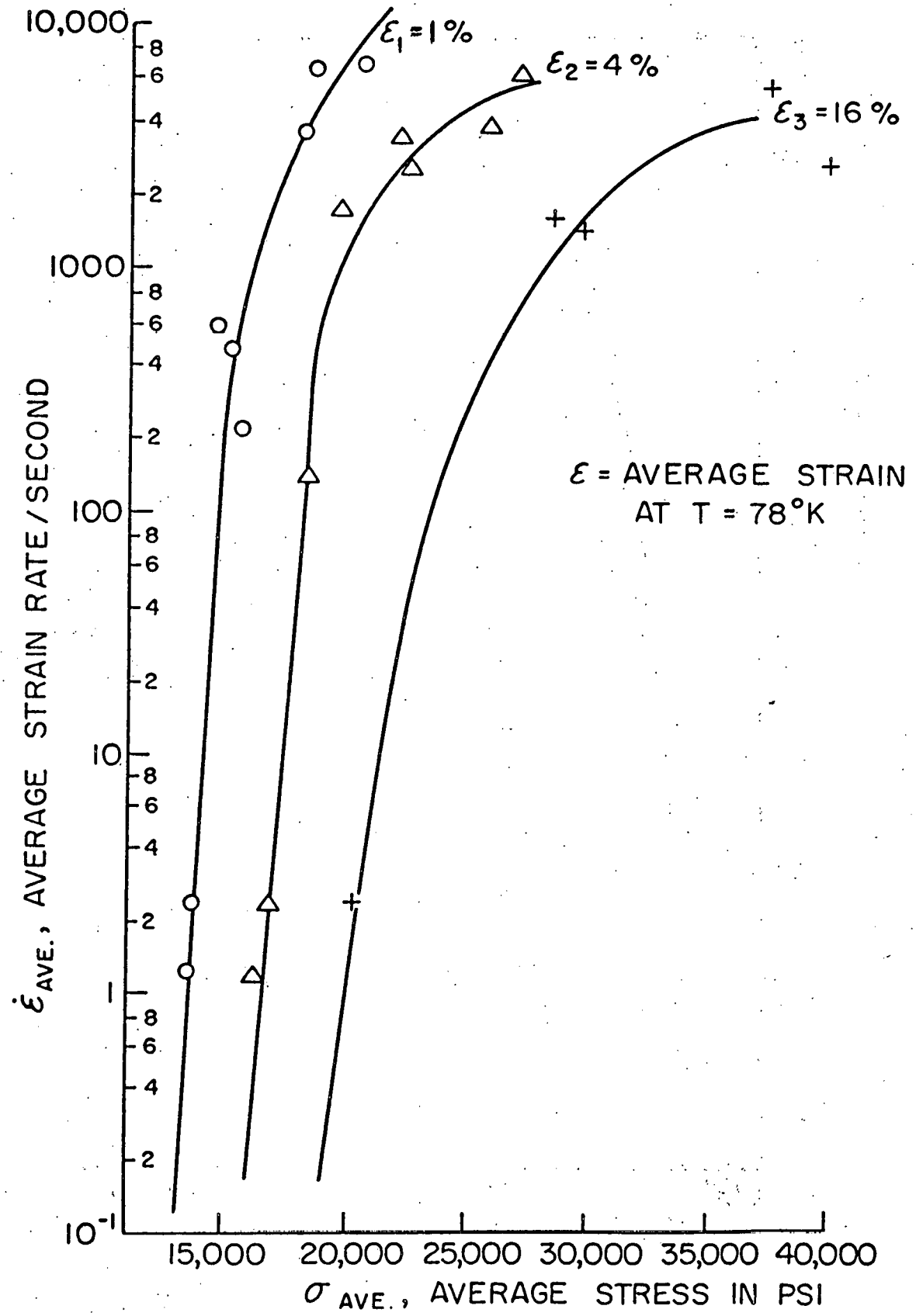

FIG. 8 EFFECT OF STRESS ON STRAIN RATE AT CONSTANT STRAIN (8).

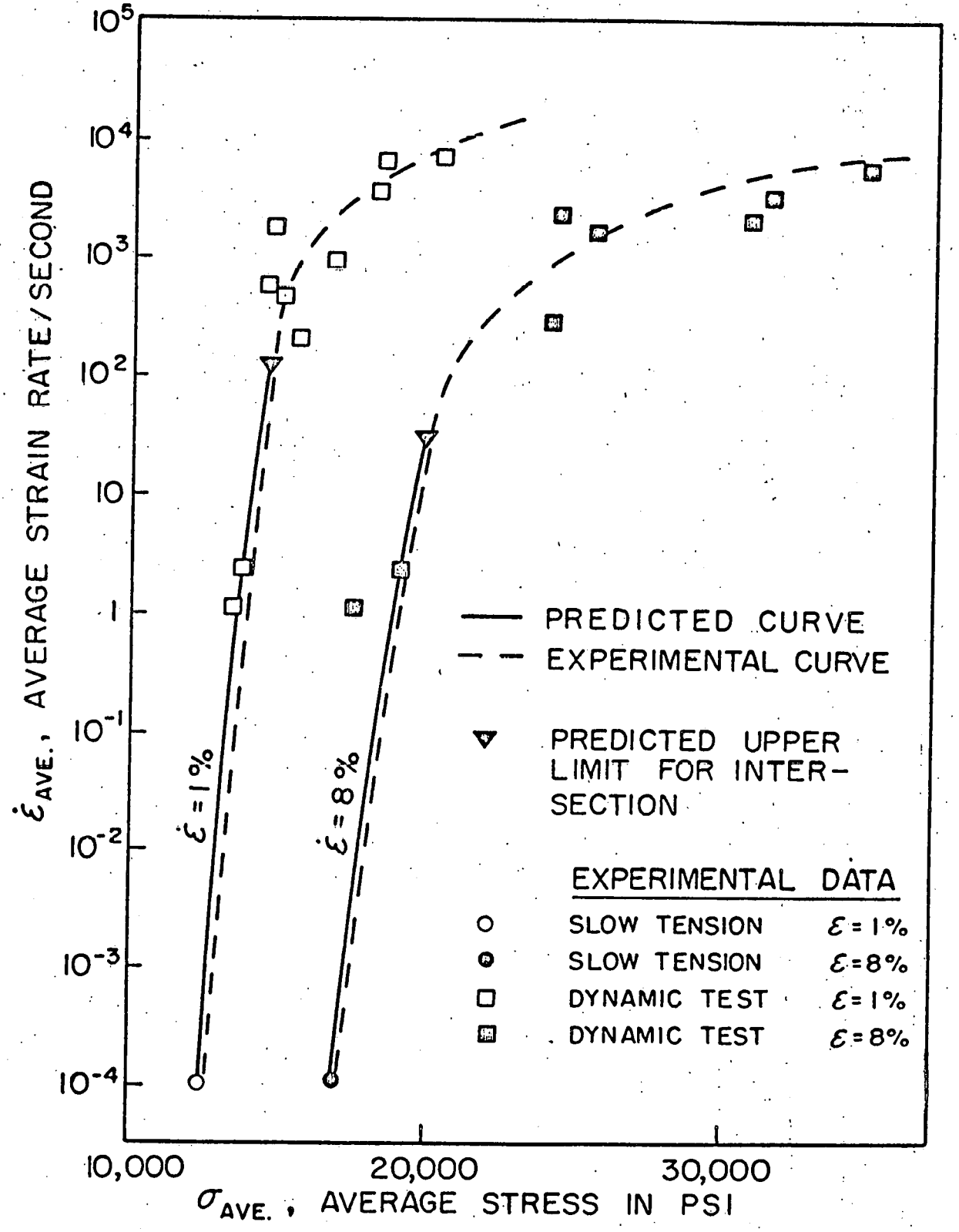

FIG. 9. PREDICTION OF THE DYNAMIC PLASTIC BEHAVIOR IN THE INTERSECTION REGION FOR PURE Al AT T = 77 °K.

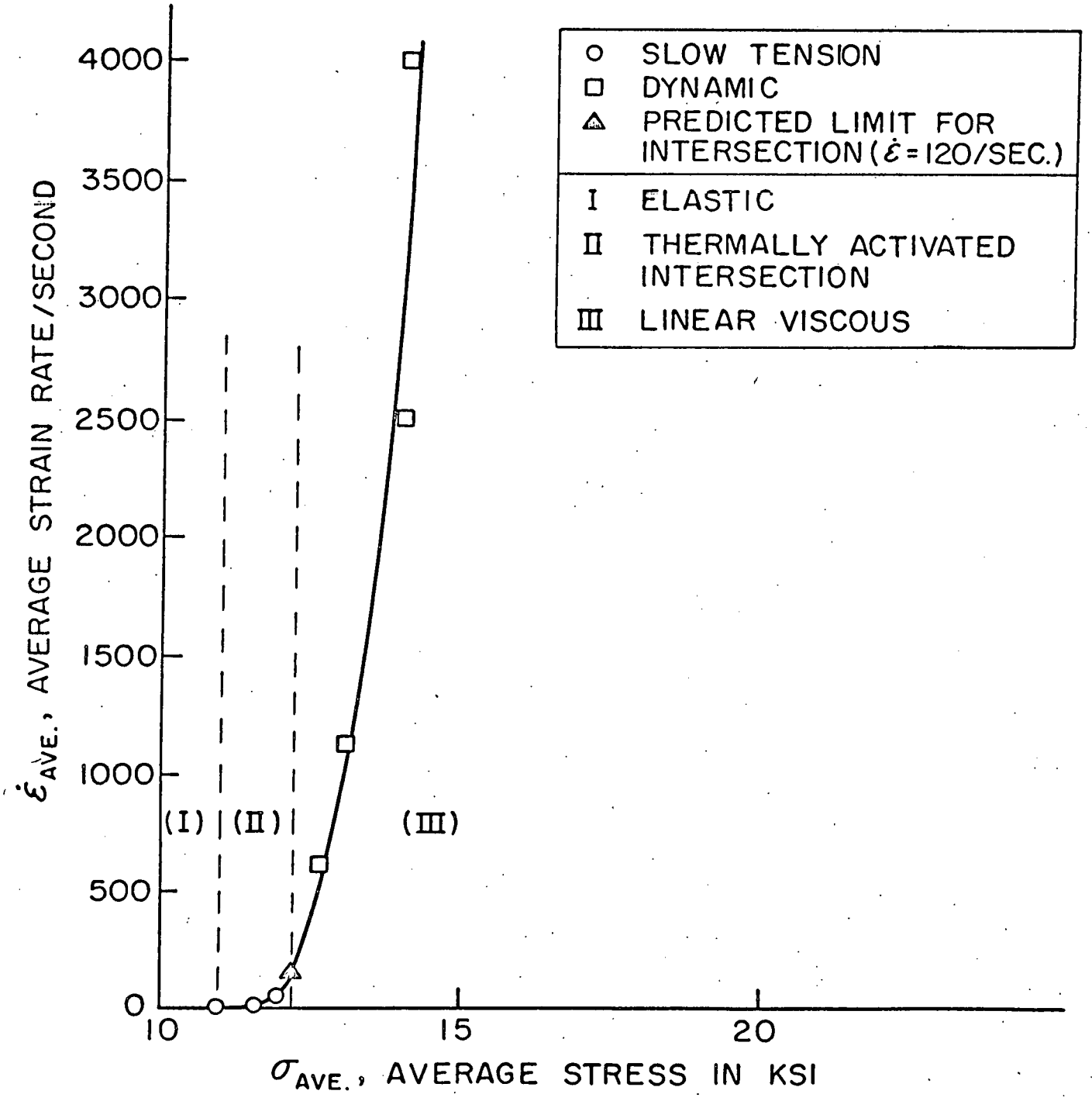

FIG. 10. EFFECT OF STRESS ON THE STRAIN RATE IN DYNAMIC TESTS IN PURE Al AT 295°K.

DO not reproduce